KONA Powder and Particle Journal No. 38 (2021) 26–41/https://doi.org/10.14356/kona.2021017 Review Paper

Static and Dynamic Stickiness Tests to Measure Particle Stickiness †

Erik J.G. Sewalt, Fuweng Zhang, Volkert van Steijn, J. Ruud van Ommen and Gabrie M.H. Meesters*

Department of Chemical Engineering, Delft University of Technology, The Netherlands

Abstract

Sticking of particles has a tremendous impact on powder-processing industries, especially for hygroscopic amorphous powders. A wide variety of experimental methods has been developed to measure at what combinations of temperature and moisture content material becomes sticky. This review describes, for each method, how so-called stickiness curves are determined. As particle velocity also plays a key role, we classify the methods into static and dynamic stickiness tests. Static stickiness tests have limited particle motion during the conditioning step prior to the measurement. Thus, the obtained information is particularly useful in predicting the long-term behavior of powder during storage or in packaging. Dynamic stickiness tests involve significant particle motion during conditioning and measurement. Stickiness curves strongly depend on particle velocity, and the obtained information is highly relevant to the design and operation of powder production and processing equipment. Virtually all methods determine the onset of stickiness using powder as a starting point. Given the many industrial processes like spray drying that start from a liquid that may become sticky upon drying, future effort should focus on developing test methods that determine the onset of stickiness using a liquid droplet as a starting point.

Keywords: stickiness, powders, caking, glass transition temperature, sintering

1. Introduction

Sticking of particles has a tremendous impact on numerous industries that process powders. Sticking can cause several issues, such as fouling and blockage of equipment, or caking of stored powder. It can also be used advantageously to produce agglomerates with beneficial properties. Why, how, and when particles stick together are critically important questions. In this review, we focus on the 'when' question by reviewing the experimental methods commonly used to determine the conditions under which sticking occurs. We hereby focus on the stickiness of hygroscopic amorphous powders, which play a major role in the food industry (Boonyai et al., 2004). Crystalline materials, which may also stick, but through a different mechanism (Kamyabi et al., 2017), are beyond this review's scope.

Whether two particles stick depends on their material and a wide variety of parameters, including their temperature, and moisture content. A common way to characterize the stickiness of a material is to map the stickiness based on the environmental temperature and the moisture content. The moisture content can be described in terms of the particle's water mass fraction (x_w), or the equilibrium environmental relative humidity (RH). The part of the parameter space for which the material is sticky is called the sticky region, which is bounded by the so-called sticky-point curve, $T_1(x_w)$, and the so-called tack boundary, $T_2(x_w)$, as illustrated in **Fig. 1**. Besides the environmental parameters, this map also illustrates the particle's material properties in the form of a boundary between the glassy state and the rubbery state, known as the glass transition temperature, $T_g(x_w)$. The rubbery state has some overlap with the sticky region, and with further hydration becomes the liquid state (Roos, 2002). While particles are non-sticky in the glassy state, material properties, especially viscosity, drastically change upon transitioning to the rubbery state. Hence, the curves represented by the differences $T_1(x_w) - T_g(x_w)$ and $T_2(x_w) - T_g(x_w)$ are two meaningful measurements of the sticky-region that include the influence of temperature, moisture content, as well as the material. The distance between the sticky-point curve $T_1(x_w)$ and the glass transition curve $T_g(x_w)$ often slightly depends on x_w (Palzer, 2005). Therefore, the onset of stickiness is commonly reported as a constant critical deviation from $T_g(x_w)$, denoted as $(T - T_g)_c$.

† Received 5 June 2020; Accepted 11 August 2020
J-STAGE Advance published online 19 September 2020
* Corresponding author: Gabrie M.H. Meesters;
Add: van der Maasweg 9, 2629HZ Delft, The Netherlands
E-mail: G.M.H.Meesters@tudelft.nl
TEL: +31-15-278-5501

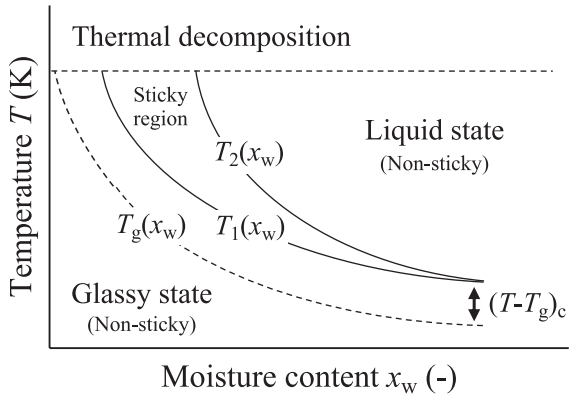

Fig. 1 Map of temperature and moisture content showing the region in which a material is considered sticky. This region is enveloped by the sticky-point curve ($T_1(x_w)$), the tack boundary ($T_2(x_w)$), and the temperature above which the material decomposes. The sticky-point curve and tack boundary are often reported with respect to the glass transition temperature of the material (dashed line), which separates its glassy state from its liquid state. The difference $T_1(x_w) - T_g(x_w)$ is in literature more commonly referred to as $(T - T_g)_c$. Figure is modified from Lockemann (1999) and Kudra (2003).

Experimental stickiness tests generally aim to determine the sticky-point curve or the tack boundary by measuring stickiness for different temperatures and moisture contents. While most methods approach the sticky region from the glassy state to find $T_1(x_w) - T_g(x_w)$, a limited number of methods approach the sticky region from the liquid state to find $T_2(x_w) - T_g(x_w)$. Although the tack boundary is less well understood, it is known that the change in behavior is less sharp than near the sticky-point curve (Kudra, 2003). While the measured parameter may differ between the experimental methods, what all methods have in common is that they follow two steps: (1) a conditioning step, where the material is subjected to a specified temperature T and humidity RH for a certain time window and (2) a measurement step where the stickiness of the powder is measured (Boonyai et al., 2004). Whereas these steps are separated for some methods, they are intertwined for others. Hence, not only the duration of conditioning influences the sticky region's boundaries but also the used measurement method. While the influence of conditioning time is well understood (Kamyabi et al., 2017), the influence of particle motion in the conditioning and/or measurement step on the boundaries of the sticky region is still unclear. For skim milk powder, one of the most abundantly tested materials, a wide range for $T_1(x_w) - T_g(x_w)$ has been reported. For particles that are static during the conditioning step, values as low as 8 °C were reported for $T_1 - T_g$ (Verdurmen et al., 2006). By contrast, values as high as $T_1 - T_g = 63$ °C were reported for particles moving at tens of meters per second (Walmsley et al., 2014).

Following Verdurmen et al. (2006), we therefore distinguish between two classes of methods in this review. The first class is where the particles can be considered static during conditioning (not set in continuous motion through external means). The second class is where the particles are moving during conditioning. We refer to the first class of methods as *static stickiness tests* and to the second class as *dynamic stickiness tests*.

This review aims to provide an overview of the available methods to measure stickiness. As static stickiness tests, we describe various visual observation tests, the shear test, the penetration test, and the blow test. As dynamic stickiness tests, we describe the sticky-point test, the fluidized bed test, the particle gun, the cyclone test, the optical test, and the probe test. For each method, we describe how it can be used to determine either the sticky-point curve $T_1(x_w)$ or the tack boundary $T_2(x_w)$ of the sticky region. Additionally, we describe what we view to be the method's best application in industry. The overview of methods shows that particle velocity plays a significant role in the measured boundaries of the sticky region, illustrating the importance of choosing the most appropriate method for the application in mind.

2. Glass transition temperature

The glass transition temperature T_g marks the temperature where an amorphous material transitions from a glassy state to a rubbery state upon increasing temperature. While both states are fundamentally a liquid, the behavior of the glassy state is solid-like, being hard and brittle, and the rubbery state behaves like a highly-viscous liquid. The nature of the glass transition is the molecular freedom of movement, which is restricted in the glassy state (Roos, 2002).

The most common method to experimentally determine T_g is using differential scanning calorimetry (DSC), although several other methods are available (Li et al., 2019). In DSC, the T_g is found by subjecting the material in the glassy state to a temperature ramp and measuring the specific heat capacity. The specific heat capacity shows a characteristic change during the glass transition (Hogan et al., 2010; Roos, 2010). By repeating the experiment at different x_w, the curve for $T_g(x_w)$ shown in **Fig. 1** can be experimentally constructed. Similarly, dynamic vapor sorption (DVS) can be used to measure the vapor sorption characteristics by applying a ramp in relative humidity at a fixed T while measuring the sample's mass. In the glassy state, water sorption only occurs at the surface, while the rubbery state also allows for bulk sorption, such that a characteristic change in the water sorption rate is observed at T_g (Burnett et al., 2004).

The glass transition temperature can also be estimated theoretically, for example using the Gordon-Taylor or Couchman-Karasz equation. The Gordon-Taylor equation can be used to determine the influence of water on the glass transition temperature $T_g(x_w)$ of a dry powder, based on the glass transition temperature of the anhydrous powder ($T_{g,s}$)

and pure water ($T_{g,w}$), and the weight fraction of moisture, x_w, as

$$T_g(x_w) = \frac{(1-x_w)T_{g,s} + kx_wT_{g,w}}{(1-x_w) + kx_w} \quad (1)$$

with $T_{g,w} = -135$ °C (Roos, 2002). The constant k is often calculated from the densities ρ, $T_{g,s}$, and $T_{g,w}$ as $k = (\rho_s T_{g,s})/(\rho_w T_{w,s})$ (Katkov and Levine, 2004; Simha and Boyer, 1962). The Couchman-Karasz equation, while similar to Eq. (1), is based on thermodynamic additivity of specific heat capacity. Although different versions are reported, the so-called 'modified' version is found when using $k = \Delta C_{p,w}/\Delta C_{p,s}$ in Eq. (1). The changes in heat capacity ΔC_p at T_g can be found using DSC (Sochava, 1997). For $\Delta C_{p,w}$, 1.94 J K^{-1} g^{-1} is often used (Katkov and Levine, 2004; Roos, 2002). Katkov and Levine 2004 showed that the modified version of the Couchman-Karasz equation overestimated the T_g of mixtures and underestimated the plasticizing effect of water while they obtained a better fit using the so-called 'original' Couchman-Karasz equation

$$\ln(T_g) = \frac{(1-x_w)\ln(T_{g,s}) + kx_w\ln(T_{g,w})}{(1-x_w) + kx_w} \quad (2)$$

While the Gordon-Taylor and Couchman-Karasz equations are suitable for most simple systems and can be used to construct the curve for $T_g(x_w)$ in **Fig. 1**, they should be used with caution when considering complex mixtures (Katkov and Levine, 2004).

The glass transition temperature servers as a natural reference in the stickiness map and allows one to compare the stickiness of different type of materials. Similarly, the T_g serves as a reference in an attempt to come to a universal predictive equation of the dynamic viscosity in the rubbery state. The Williams-Landel-Ferry (WLF) equation relates the viscosity of a material to the distance from the T_g-curve ($T - T_g$) as

$$\log_{10}\frac{\eta}{\eta_g} = \frac{C_1(T-T_g)}{C_2 + (T-T_g)} \quad (3)$$

with C_1 and C_2 two constants and η_g the viscosity at the glass transition temperature. While the WLF equation is often considered to be valid for temperatures up to $T_g + 100$ °C (Lomellini, 1992; Williams et al., 1955), it is only valid if correct values for the constants and η_g are chosen. Values of η_g are typically in a range between 10^{11} Pa s to 10^{14} Pa s (Downton et al., 1982; Katkov and Levine, 2004; Murti et al., 2010; Palzer, 2005; Paterson et al., 2015; Wallack and King, 1988). Recently, the glass viscosity of freeze dried amorphous lactose was measured to be 1.1×10^{14} Pa s, although the authors suggest that further confirmation is required (Paterson et al., 2015). The wide variety of reported constants suggests that there is no universal set valid for different types of materials and different temperatures. Nevertheless, (C_1, C_2) = (–17.44, 51.6 K) as originally reported by Williams et al. (1955), are often considered to be universal (Aguilera et al., 1993; Murti et al., 2010; Palzer, 2005; Schulnies and Kleinschmidt, 2018; Wallack and King, 1988). Peleg (1992) found that these constants give large deviations when $T - T_g > 20$ °C, and suggested (C_1, C_2) = (–10.5, 85.6 K), which better matched the experimental trend for the η_g of amorphous lactose measured by Paterson et al. (2015). However, (C_1, C_2) = (–8.86, 101.6 K) also provided a good fit to other experimental data (Dagdug and García-Colín, 1998; Ferry, 1980). Others use material-specific constants, such as (C_1, C_2) = (–14.5, 36.4 K), which were fitted for skim milk powder (Walmsley et al., 2014). Since the WLF equation is exponential, care should be taken in the choice of the constants when using the WLF equation to predict the dynamic viscosity. To illustrate the importance of this choice for a prototypical case ($T - T_g = 20$ °C and $\eta_g = 10^{12}$ Pa s), the constants by Williams et al. (1955) give $\eta = 1.3 \times 10^7$ Pa s, while the constants by Peleg (1992) gives $\eta = 1.0 \times 10^{10}$ Pa s, which is a difference of three orders of magnitude. As there are currently no clear rules of thumb on the selection of constants, we suggest that best practice would be to fit C_1 and C_2 to experimentally measured viscosity data.

The direct relation between viscosity and $T - T_g$ through the WLF equation leads to the natural question whether viscosity can be used as a predictor for stickiness. The success of viscosity as a predictor is expected to depend on the dominant mechanism of adhesion. For hygroscopic amorphous powders close to T_g, sticking is expected to occur primarily through immobile liquid bridging or viscoelastic deformation (Palzer, 2005). In case immobile liquid bridging primarily causes sticking, we generally expect viscosity to be more meaningful than when viscoelastic deformation primarily causes sticking. More specifically, using sintering theory by Frenkel (1945) and classic viscoelastic contact models, Palzer (2005) could predict the critical $T - T_g$ needed for sticking. However, this model did not successfully predict sticking of high velocity particle gun experiments (Murti et al., 2010). A contact model for adhesive elastic particles showed better results when predicting the critical $T - T_g$ for high velocity collisions (Walmsley et al., 2014). The mentioned works strongly suggest that viscoelasticity should be accounted for when predicting $(T - T_g)_c$ for collisions of particles in motion, and that the observed $(T - T_g)_c$ is a result of the colliding material's rheological behavior and the collision's kinetics.

3. Static stickiness tests

Testing stickiness of powders using static stickiness tests follows a general protocol. First, a powder bed is compressed under a stress σ to cause a certain amount of consolidation (**Fig. 2a**). Second, the powder is conditioned

by exposing it to an environment of controlled temperature and relative humidity (**Fig. 2b**). The duration of this conditioning step can be adjusted. When sufficiently long, the powder's moisture content is in thermodynamic equilibrium with the moisture in the environment such that x_w and *RH* are related through a vapor sorption isotherm. Third, a measurement is performed on the conditioned powder (**Fig. 2c**). Prior to the measurement, the powder can be considered static with little movement of the particles. Therefore, we refer to this class of tests as static stickiness tests, which are deliberately different from the dynamic stickiness tests in which the particles are actively set in continuous motion during the conditioning and measurement step. Next, we describe the different static stickiness tests.

3.1 Visual observation

The most straightforward form of analysis is through visual observation. Typically, a sample with a specified dry matter content is placed in a closed container. After conditioning it at a given temperature, the container is turned upside down to see whether any particles are stuck to the bottom. This procedure is repeated at different temperatures until particles noticeably stick to the bottom, which is identified as the sticky-point temperature (Palzer, 2005). By repeating this procedure for different moisture contents, the sticky-point curve $T_1(x_w)$ in **Fig. 1** can be constructed. An alternative visual observation test is one in which the powder's temperature is increased stepwise while observing changes in the appearance of the powder bed (Tsourouflis et al., 1976; Verdurmen et al., 2006).

3.2 Shear test

Shear tests are used to characterize powder stickiness by measuring the powder's response to shear stress. Two common approaches are uniaxial compression and shearing in shear cells. The uniaxial compression approach consolidates the bed with normal stress σ and then compresses along one axis until failure. The failure stress σ_f for different values of σ gives a yield locus that can be used to find the unconfined yield strength σ_c by drawing a Mohr circle starting at $\sigma = 0$ Pa (Schulze, 2008). The unconfined yield strength σ_c is used as the parameter for bed strength and can be determined for different environmental *T* and *RH* (Fitzpatrick et al., 2007b; Hartmann and Palzer, 2011). In order to find a sticky-point curve $T_1(x_w)$, a critical bed strength, which is characteristic for a sticky powder, must be determined first. It can be empirically determined before testing using the same or comparable materials (Palzer and Zürcher, 2004).

Similarly to uniaxial compression, shear cells can be used to determine σ_c and acquire $T_1(x_w)$ by defining a critical σ_c for the bed strength of a sticky powder (Hartmann and Palzer, 2011; Schulnies and Kleinschmidt,

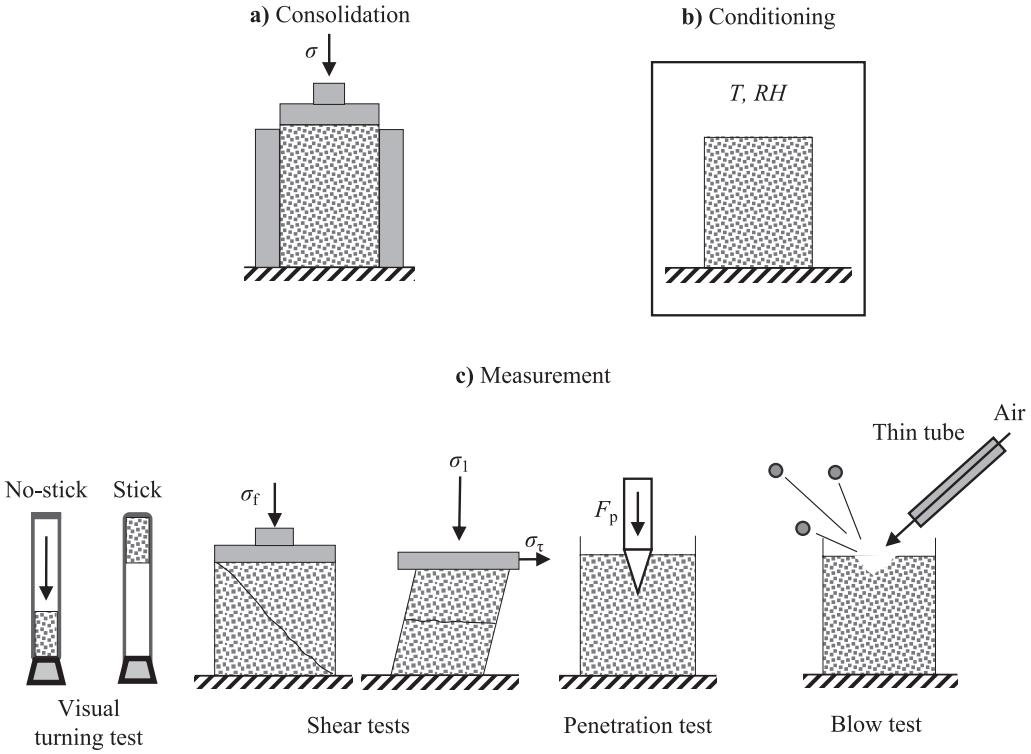

Fig. 2 An overview of the static stickiness tests. **a)** In the consolidation step, the powder is compressed under a stress σ. **b)** In the conditioning step, the powder is subjected to temperature *T* and relative humidity *RH* for a specified duration. **c)** The measurement of stickiness proceeds differently per test.

2018). However, shear cells improve on result consistency by preshearing before measuring the failure stress. Preshearing to steady-state at normal stress σ_1 eliminates any stress history, for example, due to filling (Schulnies and Kleinschmidt, 2018). After preshearing, the shear stress is reversed to reduce the shear stress to zero. Subsequently, the sample is sheared to failure while measuring shear stress σ_τ under normal stress σ_2 so that $\sigma_1 < \sigma_2$ (overconsolidation), which ensures a peak is observed for the failure stress (Schulze, 2008). By shearing to failure at different σ_2 while preshearing at identical σ_1 a yield locus can be found. From this point on, the acquisition of σ_c and $T_1(x_w)$ is similar to uniaxial compression.

Besides acquiring the sticky-point curve, shear tests have other commonly used applications related to stickiness and powder cohesion. Shear tests are commonly used to quantify the powder flowability. The flowability is described in terms of the flow function, which is the inverse slope in a plot of unconfined yield strength σ_c versus normal stress σ (Fitzpatrick et al., 2007b; Jenike, 1964; Papadakis and Bahu, 1992; Schulze, 2008). Shear cells can also be used to measure wall friction. This is done by replacing the bottom ring of a shear cell with the wall material. When choosing the wall material similar to industrial surfaces or packaging materials, the adhesion of powder to these substrates can be measured (Papadakis and Bahu, 1992; Schulze, 2008).

Commonly used examples of shear cells are the manual Jenike shear cell (Jenike, 1964), the automated Schulze ring shear test (Schulnies and Kleinschmidt, 2018), or the more recent Freeman FT4 Powder Rheometer (Freeman, 2007) and Anton Paar MCR rheometers (Anton Paar GmbH, 2020; Groen et al., 2020). Conveniently, both the Freeman and Anton Paar powder rheometers can quickly change environmental T and RH independently through powder bed aeration with conditioned airflow (Freeman, 2007; Groen et al., 2020; Mitra et al., 2017). Besides uniaxial compression and shear cells, other types of shear tests for measuring flowability have been reported (e.g., Warren Spring cohesion tester, Peschl shear cell). These were not described as their application to find $T_1(x_w)$ was not found in literature (Pasley et al., 1995).

3.3 Penetration test

Penetration tests are similar to the uniaxial compression tests, but use a puncher with a diameter of 1 mm to 2 mm to penetrate the powder bed to a preset depth (Knight and Johnson, 1988). Measurement of the required penetration force F_p, which is a measure for bed strength (Özkan et al., 2002; 2003), is done after conditioning at a fixed T and RH for a given time. Through repetition, while varying these conditions, the sticky-point curve $T_1(x_w)$ is found for the combinations of T and RH, where the measured F_p equals a predetermined critical value for which the powder is considered sticky (Özkan et al., 2003).

3.4 Blow test

The blow test uses a small thin tube to blow air at a powder bed surface. The tube is placed millimeters above the surface at an angle of 45°. The airflow through the tube is increased until particles dislodge from the surface of the conditioned powder bed, which is the endpoint of the blow test. The flow rate of air at which particles start dislodging is a measure for bed strength (Paterson et al., 2001). The sticky-point curve $T_1(x_w)$ is found at the T and RH where the airflow to dislodge particles reaches a predetermined critical value for which the powder is considered sticky (Foster et al., 2005; Paterson et al., 2005).

A benefit of the blow test is the ability to test multiple times without needing to repeat the consolidation and conditioning step. The powder bed sits on a distributor plate, which sections the powder into multiple parts with an equal amount of powder. Each section of powder is conditioned with the same T and RH and can be measured separately by rotating the thin tube. Therefore, the blow test is convenient when interested in temporal measurements, such as determining the rate of bed strength increase (Paterson et al., 2005).

3.5 Comparison of tests

While simplicity is a strength of the visual observation tests, it is also their greatest weakness. The accurate detection of the sticky-point temperature relies on the observer's experience. Based on caking theory, we expect that visible changes in powder properties occur after a high degree of agglomeration has taken place (Kamyabi et al., 2017). Hence, human observers can miss the onset of stickiness, which would cause an over-prediction of the sticky-point temperature. The onset of stickiness can be more precisely quantified with the other tests. Based on the literature, we find that shear tests are more accurate than penetration tests, with less scatter of data and time consolidation effects that are easier to detect (Knight and Johnson, 1988; Schwedes, 2003). Based on these findings, we recommend using uniaxial compression or shear cells instead of penetration tests, in line with Knight and Johnson (1988), who recommended to only use penetrometry in support of shear cell experiments. While shear tests are applied to the bulk of the powder, the blow test is applied to the powder's surface, suggesting that the blow test mostly tests the surface conditions. Blow tests nevertheless create channels in the powder bed (Billings et al., 2006; Paterson et al., 2005), indicating that the bulk is strongly affected by blow test. Hence, we expect that blow tests can be used to determine (bulk) stickiness, similarly to the shear tests. An advantage of the shear tests over the blow test is that the compression

during consolidation can be maintained during conditioning, while an advantage of the blow test over the shear tests is that multiple measurements can be performed without having to repeat the consolidation and conditioning steps.

The shear, penetration, and blow tests can be used to quantify bed strength for different T and RH based on the measured parameter (yield strength, penetration force, flow rate). To, in turn, relate bed strength to stickiness, a predetermined value of the critical bed strength is required at which the powder of interest is considered sticky. A way to overcome having to predetermine a critical bed strength is by considering the temporal behavior. Experiments with the blow test, for example, show an initial linear increase of bed strength with time (Foster et al., 2006; Paterson et al., 2005). Similar experiments with shear cells are time-consuming since each test requires repetition of consolidation and conditioning, but suggest a similar linear increase of bed strength with time (Fitzpatrick et al., 2007a; 2007b; 2008). By measuring the rate (i.e., slope) of increase for a range of $T - T_g$, one can infer the sticky-point curve $T_l(x_w)$ by plotting the rate versus $T - T_g$ and extrapolating to arate of zero. In case the critical bed strength is not available a priori, studying the temporal behavior to determine the rate of bed strength increase as a function of $T - T_g$ provides a means to construct the sticky-point curve $T_l(x_w)$.

3.6 Application areas of static stickiness tests

Generally, the static stickiness methods are useful in predicting the long-term behavior of powder during storage, transport, or in packaging. In these situations, particles may stick together under the influence of humidity in a process known as caking. This process comprises multiple steps. Firstly, environmental conditions cause particle surfaces to become viscous. Contacting liquid particle surfaces become connected through liquid bridges. Secondly, the liquid bridges that formed grow in size, increasing powder cohesion. Thirdly, the pores that existed between particles disappear as the liquid fills up the pores (Kamyabi et al., 2017). During the caking process, the bed strength initially increases with time until a maximum value is achieved. As the process continues, the bed strength starts to decrease, attributed to partial crystallization of material to non-sticky crystals (Fitzpatrick et al., 2007b), as well as a decreased liquid bridge viscosity due to increased liquid adsorption (Hartmann and Palzer, 2011). Static stickiness tests are particularly suitable for assessing the progress of caking by monitoring bed strength as a function of time. Shear tests are particularly useful because they can emulate storage environment conditions in a warehouse or transport vehicle by maintaining a certain level of compression during conditioning and measurement. Using shear cells where the powder can be sheared against a wall material is also applicable to measure powder stickiness in food packaging.

4. Dynamic stickiness tests

The class of dynamic stickiness tests covers the tests where particles are not static during conditioning, but set in continuous motion through external means. This introduces particle velocity or contact time between particles as an additional relevant parameter. An overview of dynamic stickiness tests is listed in **Table 1**, showing the measured parameter and the most suitable application. Most dynamic stickiness tests approach the sticky region from the glassy state, while just a few approach it from the liquid state.

4.1 Sticky-point test

The sticky-point test is the earliest reported method to measure stickiness, hence the name (Lazar et al., 1956). This test has also been referred to as a propeller-driven test (Boonyai et al., 2004). As shown in **Fig. 3**, the device

Table 1 List of methods to measure dynamic stickiness

Method	Measured parameter	Application
Sticky-point test	Torque	Powder mixing
Fluidized bed	Bed collapse/Pressure drop	Fluidized beds:
		Preventing bed collapse
		Granulation
Particle gun	Deposited mass	Pneumatic transport
		Cyclones
Cyclone test	Visual change	Pneumatic transport
		Cyclones
		Fluidized beds
Optical test	Scatter intensity	Versatile application, opaque powder
Probe test	Tensile force	Droplet evaporation

uses a container in which a powder with known moisture content x_w is placed. The sample container is submerged in a heating medium to control the powder's temperature. The sample is continuously stirred at fixed angular velocity with a stirring device, and the required torque τ is measured. Typically, a temperature ramp is imposed where the temperature is slowly increased until the powder transitions from the glassy to the rubbery state. Above T_g, the cohesive forces increase. Further increase of the temperature leads to particles sticking together, leading to a sharp increase in the required τ. The temperature where this sharp increase is observed is identified as the sticky-point temperature. By repeating the test with different x_w, the sticky-point curve $T_1(x_w)$ can be found.

Detection of the sticky-point in the earliest versions relied on manual stirring. When the stirring had become noticeably more demanding, the sticky-point was reached (Downton et al., 1982; Lazar et al., 1956). More accurate detection methods use automatic stirrers or shear cells equipped with stirrers, which record the τ required for stirring (Özkan et al., 2002; Wallack and King, 1988). Recently, the method has been further improved by utilizing aeration in an Anton Paar rheometer equipped with a propeller (Groen et al., 2020). The option to aerate the powder is used to fluidize the powder, which occurs at a sufficiently high airflow velocity. The powder conditions are controlled by changing the T and RH of the airflow, instead of using a heating medium surrounding the container. The propeller stirs the fluidized powder and measures the required τ. The required τ is substantially smaller than without fluidization, although the rheometers are sufficiently sensitive (Groen et al., 2020). The benefit of aeration or fluidizing is that environmental conditioning occurs rapidly by changing the air's temperature and humidity. In our view, this makes the sticky-point test combined with fluidizing the powder a promising method for measuring dynamic stickiness, both in terms of accuracy and a shorter experimental time.

Besides applying the sticky-point test to free-flowing powder, it has also been used to measure the stickiness of drying liquids. Hence, instead of determining the sticky-point curve $T_1(x_w)$, the tack boundary $T_2(x_w)$ is determined. Kudra (2003) used a laboratory batch dryer equipped with a stirrer to measure the stickiness of drying sludge. They found that the temperature where the torque substantially increased was different from the $T_1(x_w)$ that is found when approaching from the glassy state. The conclusion was that most materials have a sticky-region in which they are sticky (Kudra, 2003).

4.2 Fluidized bed

As discussed for the sticky-point test, the fluidization of powder reduces the required conditioning time. However, because powder fluidization is highly sensitive to powder cohesiveness, the fluidized bed in isolation is also suitable to measure stickiness. In a fluidized bed, which is shown in **Fig. 4**, a powder bed sits in a column while airflow is applied at the bottom. Fluidization causes expansion of the powder bed so that the powder displays fluid-like behavior with a high degree of mixing. The sticky-point curve's acquisition goes as follows: The T or RH of the fluidizing air is increased stepwise. Most commonly, a RH ramp is used at a fixed T by increasing the airflow's humidity. As the cohesiveness increases, there is a point where the fluidized bed collapses (defluidization). The conditions where the collapse of the powder bed is observed, visually, or using pressure drop measurements, is the sticky-point T_1 (Palzer, 2005; Verdurmen et al., 2006). By repeating the RH ramp at different temperatures, the sticky-point curve $T_1(x_w)$ can be drawn.

In many cases, fluidized bed collapse is detrimental when it occurs. Hence, much research has been done on the detection and prevention of bed collapse (Bartels et al., 2008). Methods such as the attractor comparison method can be used to detect early changes in the bed that indicate an upcoming collapse (Van Ommen, 2001) and have been used to determine the sticky-point curve $T_1(x_w)$ (van

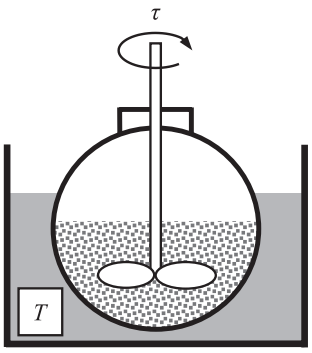

Fig. 3 A sticky-point test. A powder with known moisture content is placed in a temperature-programmable water bath. The powder is stirred at a fixed angular velocity, and the required torque τ is measured.

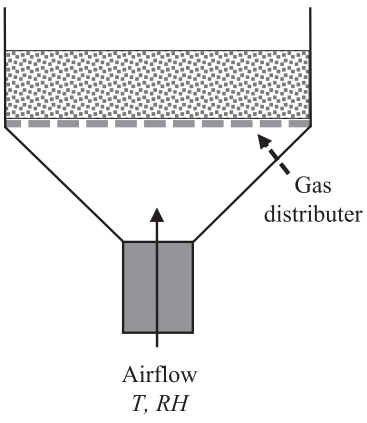

Fig. 4 A fluidized bed test. The humidity or temperature of the conditioned airflow is increased stepwise until the powder bed collapses.

der Knaap, 2006; Verschueren et al., 2007). When such detection methods are implemented, the sensitivity of the fluidized bed as a stickiness test is expected to be high.

4.3 Particle gun

The particle gun has been designed to measure the sticking of high-velocity particles to a wall and is shown in **Fig. 5**. It is a duct through which conditioned air is flowing at high velocity with a target plate at the far end of the duct. For each experiment, a sample of approximately 25 g powder is introduced into the duct. The particles become entrained in the conditioned air-jet shortly until eventually impacting the target plate. Due to the short exposure of particles to the air, the particle gun relies heavily on the rapid acclimation of the powder surface to environmental conditions. The short acclimation time has consequences for liquid bridge formation as the thin surface region that has adsorbed vapor limits their potential width (Murti et al., 2010). The measured parameter is the percentage of injected powder deposited on the target plate. Plotting this parameter versus $T - T_g$ shows negligible 0 % deposition until a critical value of $T - T_g$ is reached. Above this temperature, deposition is observed and increases linearly with $T - T_g$. The temperature where deposition starts increasing is taken as $T_1(x_w)$ (Zuo et al., 2007).

4.4 Cyclone test

The cyclone test, shown in **Fig. 6**, uses a cyclone in which conditioned air is circling (Boonyai et al., 2002). When the air is at a steady-state, approximately 1 g of powder is injected at the top of the cyclone. When conditions are such that the powder becomes sticky, particle lumps and powder deposition on the cyclone are observed within minutes. Longer experimental times lead to full immobilization of the powder. The experiment starts at a low *RH* of the air and is increased stepwise until lumping and deposition are observed visually, which marks a point on the sticky-point curve $T_1(x_w)$.

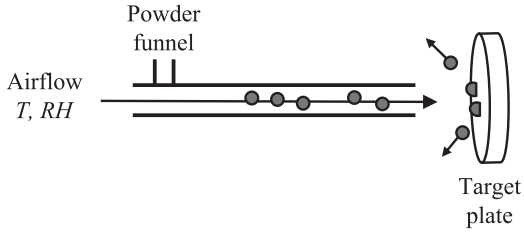

Fig. 5 The particle gun. Conditioned air flows with high velocity through an air duct. The powder is introduced through a funnel, and the entrained particles hit the target plate. Particles either bounce off or deposit on the plate.

4.5 Optical test

Lockemann (1999) proposed an optical test, shown in **Fig. 7**, which uses changes in reflectivity to determine the sticky-point curve. The proposed optical test consists of a rotating test tube containing the free-flowing powder with known (x_w). The tube is inserted into an oil bath with a programmable temperature. A near-infrared source emits light to the sample while a fiber-optical sensor records the back-scattered signal. The sensor is also immersed in the oil-bath to prevent any refraction of the signal. When particles in the tube stick together, the powder flowability changes, which is observed as a sudden change in reflectivity. This marks the sticky-point temperature T_1 (Lockemann, 1999). The experiment has to be repeated for different x_w to determine $T_1(x_w)$.

4.6 Probe test

The probe test is the only method that is solely applicable to measure stickiness when starting from the liquid state. Hence, instead of the sticky-point curve $T_1(x_w)$, the tack boundary $T_2(x_w)$ is found. The probe test can be applied to liquid films or droplets (Chen J. et al., 2008; Werner et al., 2007a). The approach for either is similar.

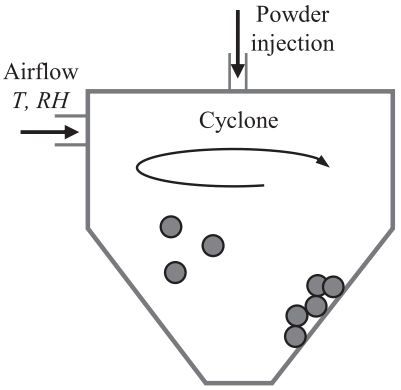

Fig. 6 A cyclone stickiness test. Conditioned airflow is used to circulate a powder sample through the cyclone. Non-sticky particles remain entrained in the cyclone, while sticky particles can agglomerate or stick to the cyclone wall.

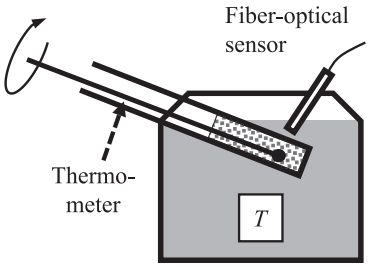

Fig. 7 The optical test. A rotating sample tube is placed in a heated water bath. A fiber-optical sensor illuminates the sample and receives scattered light. Redrawn from Lockemann (1999).

The droplet probe test is shown in **Fig. 8** and goes as follows. Droplet evaporation is monitored gravimetrically by placing the droplet on a scale (Werner et al., 2007a, 2007b). At some point during evaporation, a probe is lowered with a fixed speed to touch the droplet's surface and then retracted, also with a fixed speed, while the required force for retraction is measured. Hence, this approach is similar to a force measurement with Atomic Force Microscopy (Fabre et al., 2016). The peak tensile force F_{TU} is then determined, which is a measure of the tack, or stickiness, of the sample (Hammond, 1965; Kambe and Kamagata, 1969). By plotting F_{TU} versus drying time, a point is found where F_{TU} increases substantially, marking the tack boundary $T_2(x_w)$ with x_w determined gravimetrically based on the initial solids concentration and the measured weight loss. It should be noted that the measured F_{TU} is influenced by the probe speed and material (Adhikari et al., 2007; Green, 1942). Besides x_w, the sample's temperature T also changes during evaporation, which should be accounted for when determining $T_2(x_w)$ (Schutyser et al., 2019).

4.7 Comparison of tests

The particle gun, fluidized bed, cyclone test, and optical test use a powder as a starting point, approaching the sticky region from the glassy state to find the sticky-point curve $T_1(x_w)$. The probe test starts from the liquid state and hence can be used to determine the tack boundary $T_2(x_w)$. The sticky-point test can be used starting from the glassy or liquid state and is hence suited for determining both boundaries. The influence of inter-particle contact time was already observed for the static stickiness tests investigating caking. The longer the powder bed is subjected to environmental conditions where the powder will cake, the stronger the powder bed becomes. Control over particle motion and contact time in the dynamic stickiness tests provides a means to investigate the influence of motion within a sample on the boundaries of the sticky region.

Particle motion depends on the angular velocity of the stirrer or the container in the sticky-point and optical tests, on the air velocity in the fluidized bed, cyclone test, and particle gun, and the probe speed in the probe test. A key challenge, in comparing these tests or studying the influence of particle motion on the boundaries of the sticky region, is that particle motion largely differs in all these tests. Even for a single test at a single condition, particle motion may be heterogeneous. In a sticky-point test, for example, stirring can cause the powder to distribute inhomogeneously in the stirring vessel, e.g., due to the stirrer digging channels in the powder. Similarly, in a fluidized bed, the particle velocities are inhomogeneous, mostly due to the common occurrence of bubbling (Seville et al., 2000). Hence, quantification of the relative velocity between the particles, and the resulting inter-particle contact time, presents a challenge, apart from the particle gun where the particle impact velocity may be controlled and quantified (Murti et al., 2010; Walmsley et al., 2015; Zhao, 2009).

The clearest influence of particle motion has been observed with the particle gun, as shown in **Fig. 9**. The data by Murti et al. (2010) shows a minimal increase for $(T - T_g)_c$ with increasing v_i. The data by Walmsley et al. (2015) shows a sharp increase of $(T - T_g)_c$ with increasing v_i, although, at $v_i > 20$ m s^{-1}, the effect appears to level off. A similar trend was observed by Zhao (2009) where v_i ranged from 10 m s^{-1} to 45 m s^{-1}. These particle gun experiments show that a larger v_i shifts $T_1(x_w)$ to higher temperatures so that $(T - T_g)_c$ is increased.

The influence of particle motion also becomes apparent when different methods are compared with each other. A static method where the visual change of an SMP bed was used to find $(T - T_g)_c$ was compared with a dynamic fluidized bed method where the pressure change was used to find $(T - T_g)_c$ (Verdurmen et al., 2006). Over an

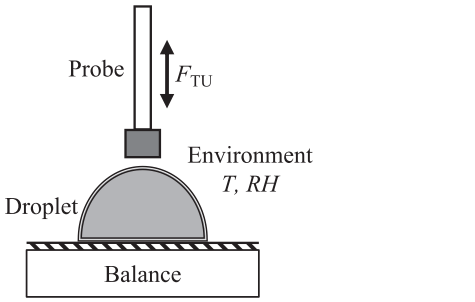

Fig. 8 The probe test. A probe is lowered until it touches the evaporating droplet. The probe retracts, and the required tensile force F_{TU} is measured. The droplet evaporation is monitored gravimetrically. Redrawn from Boonyai et al. 2004.

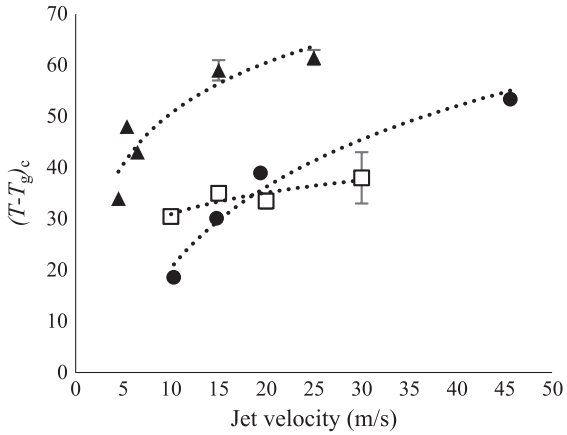

Fig. 9 Velocity-dependence of $(T - T_g)_c$ using skim milk powder and the particle gun. Triangles ▲ are data by Walmsley et al. (2015); circles ● are data by Zhao (2009), and squares □ are data by Murti et al. (2010). Note that the data cannot be directly compared between authors as different experimental settings were used. Error bars indicate the experimental range for $(T - T_g)_c$ that was reported by the respective authors. The dashed trendlines are to guide the eye.

experimental range of RH = 12 % to 30 %, the average offset of the sticky-point curve to the T_g was determined. The static test resulted in an average offset of $T - T_g$ = 13 °C and the dynamic stickiness test resulted in an average offset of $T - T_g$ = 18 °C. Another example is a comparison between the dynamic fluidized bed and particle gun tests. The $(T - T_g)_c$ was obtained for both methods using various types of skim and whole milk powder. While the results varied, for 6 out of 8 samples, the $(T - T_g)_c$ was lower for the fluidized bed by ≈ 10 °C to 15 °C. For the other two samples, the two methods provided similar results (Murti et al., 2010; Zuo, 2004). Based on these results, we strongly recommend matching the velocity of the particles in the dynamic stickiness test to the application in mind to achieve the most accurate $T_1(x_w)$.

In an attempt to further clarify the influence of particle motion on $(T - T_g)_c$, data from dynamic stickiness tests was gathered in **Table 2**. No data was found for the optical test and data for the probe test could not be used to find $(T - T_g)_c$. For each experiment, the impact velocity v_i of particle collisions was estimated. For the particle gun, the v_i was chosen as the air jet velocity. For the sticky-point test, v_i was estimated as the maximum angular velocity of the stirrer. For the fluidized bed, an average particle velocity $\hat{v}_p$ was estimated using Eq. (4), with U the superficial velocity and U_{mf} the minimum fluidization velocity (Ennis et al., 1991). The constant α was estimated from Seville et al. (2000) to be α = 0.53.

$$\hat{v}_p = \alpha(U - U_{mf}) \tag{4}$$

For the data where v_i could be estimated, no clear trend with $(T - T_g)_c$ could be found. Nonetheless, a wide range of $(T - T_g)_c$ = –5 °C to 90 °C has been reported. Further analysis indicated that, besides v_i, material and experimental differences can also play a substantial role in determining $(T - T_g)_c$, some of which is highlighted below.

Some outliers can be explained by material differences, e.g. the $(T - T_g)_c$ = 90 °C is for a skim milk powder (SMP) with 80 % protein, which is known to decrease stickiness (Hogan and O'Callaghan, 2010). Another example is the low value of –5 °C for a fluidized bed experiment using amorphous lactose. Using a range of RH = 7 % to 32 %, the results were $(T - T_g)_c$ = –5 °C to 3.8 °C with a single outlier of $(T - T_g)_c$ = 21 °C for RH = 53 %, the highest humidity tested. Amorphous lactose is known for its early onset of stickiness (Zuo et al., 2007) and crystallization (Schulnies and Kleinschmidt, 2018). We expect the latter could have played a role in the outlier as crystallization reportedly reduces liquid bridge strength (Fitzpatrick et al., 2007b).

However, even for similar materials, the deviation can be quite large. Using SMP in a particle gun with a velocity of 15 m s^{-1} the $(T - T_g)_c$ was found to be 34 °C to 36 °C by Murti et al. (2010) and 57 °C to 61 °C by Walmsley et al. (2014). Two experimental differences explained this deviation. In the experiment of Walmsley et al. (2014), the deposition was only measured for the air jet's impingement location, not for the entire target plate. Particles that stray from the jet direction move through the air with undefined T and RH. Hence, the surface conditions of stray particles cannot be accurately determined. Additionally, the target plate was heated to match the temperature of the air jet. The plate temperature T_p can play an important role and is often a relevant industrial parameter, e.g., in dryers, pneumatic ducts, fluidized beds, and cyclones (Walmsley et al., 2014). A higher T_p is known to reduce the amount of wall deposition (Chen X.D. et al., 1993). Walmsley et al. (2014) found reduced deposition for higher T_p, which was consistent regardless of the used v_i. Such wall temperature effects are also found outside of food processing, such as cold spray deposition (Khalkhali and Rothstein, 2020). The improvements of the particle gun made by Walmsley et al. (2014) show that the experimental conditions influence the resulting $T_1(x_w)$. Hence, the experimental conditions need to be accurately chosen when stickiness tests are used for predicting powder processing parameters.

4.8 Application areas of dynamic stickiness tests

The moving nature of the particles in dynamic stickiness tests makes these tests useful for predicting the behavior of powder in most of powder production and processing equipment. However, it makes them unsuitable for measuring powder caking. The application of the dynamic tests will depend on the impact velocity v_i of collisions and whether particle-particle or particle-wall collisions are tested.

The particle gun can measure the highest impact velocity of all the reviewed methods and involves particle-wall collisions. Initially, an impact velocity of 20 m s^{-1} was chosen for its similarity to industrial cyclones (Zuo et al., 2007). The high impact velocity makes it a useful method to predict stickiness for high-velocity pneumatic handling, dried material colliding with spray dryer walls, or industrial cyclones. Additionally, by changing the target plate's material or dimensions, the influence of wall material or impact angle can also be investigated (Murti et al., 2010; Walmsley et al., 2015).

The sticky-point test and fluidized bed have continuously moving powder, making these tests useful for various industrial applications involving moving powders such as powder mixing, blending, and milling. Since many industrial processes incorporate a fluidized bed, a stickiness test using fluidized powder will be most applicable to the fluidized bed itself. Limitations of the stirrer's angular velocity and the velocity of fluidization airflow make the sticky-point test and fluidized bed ill-suited for

Table 2 A selection of the reviewed literature for dynamic stickiness tests.

Material	Method	$(T - T_g)_c$ (°C)	v_i (m s^{-1})	Ref.
Sucrose & fructose	Sticky-point test	9 to 26[a]	—	Downton et al., 1982
Amorphous lactose	Fluidized bed	–5 to 21	0.055 ± 0.055[b]	Zuo et al., 2007
Amorphous lactose	Particle gun	19 to 37	20	Zuo et al., 2007
Amorphous lactose	Particle gun	36 to 40[a]	20	Paterson et al., 2007a
Coffee creamer (maltose)	Fluidized bed	10 to 20[a]	0.05 ± 0.025[b]	Groen et al., 2020
High fat cream powder	Particle gun	38	20	Paterson et al., 2007b
Low fat cream powder	Particle gun	26	20	Paterson et al., 2007b
SMP15	Fluidized bed	10	—	Hogan and O'Callaghan, 2010
SMP25	Fluidized bed	22	—	Hogan and O'Callaghan, 2010
Maltodextrin DE21	Fluidized bed	47 to 62	—	Palzer, 2005
SMP55	Fluidized bed	45	—	Hogan and O'Callaghan, 2010
SMP80	Fluidized bed	90	—	Hogan and O'Callaghan, 2010
Orange juice powder	Sticky-point test	17 to 25[a]	—	Brennan et al., 1971
SMP	Fluidized bed	14 to 23	—	Verdurmen et al., 2006
SMP	Fluidized bed	29	—	Hogan and O'Callaghan, 2010
SMP	Fluidized bed	25 to 34	0.01	Murti et al., 2010
SMP	Sticky-point test	23	0.3	Hennigs et al., 2001
SMP	Cyclone test	11.4	—	Intipunya et al., 2009
SMP $d < 45$ µm	Particle gun	8.2	10.3	Zhao, 2009
SMP $d < 45$ µm	Particle gun	14.8	19.4	Zhao, 2009
SMP $d = 45$ µm to 65 µm	Particle gun	11.6	10.3	Zhao, 2009
SMP $d = 45$ µm to 65 µm	Particle gun	23.5	19.4	Zhao, 2009
SMP	Particle gun	18.6	10.3	Zhao, 2009
SMP	Particle gun	30.1	14.8	Zhao, 2009
SMP	Particle gun	39	19.4	Zhao, 2009
SMP	Particle gun	53.4	45.6	Zhao, 2009
SMP	Particle gun	34	4.5	Walmsley et al., 2015
SMP	Particle gun	48	5.4	Walmsley et al., 2014
SMP	Particle gun	43	6.5	Walmsley et al., 2015
SMP	Particle gun	30 to 31	10	Murti et al., 2010
SMP	Particle gun	34 to 36	15	Murti et al., 2010
SMP	Particle gun	57 to 61	15	Walmsley et al., 2014
SMP	Particle gun	32 to 35	20	Murti et al., 2010
SMP	Particle gun	60 to 63	25	Walmsley et al., 2014
SMP	Particle gun	33 to 43	30	Murti et al., 2010
Tomato powder	Sticky-point test	36 to 41[a]	—	Lazar et al., 1956
White cheese powder	Particle gun	28	20	Paterson et al., 2007b
Whole milk powder	Fluidized bed	23 to 38	0.09	Zuo et al., 2007
Whole milk powder	Particle gun	38 to 61	20	Zuo et al., 2007
Whole milk powder	Sticky-point test	36 to 41[a]	1.0	Özkan et al., 2002

[a] The $(T - T_g)_c$ was not directly obtainable from the paper, instead, it was calculated using Eq. (1) and Eq. (2).
[b] A range for fluidization velocity was reported, authors did not test the influence of velocity.
SMP15: Skim milk powder with 15 % protein, similar for SMP25, SMP55, and SMP80. Ranges for $(T - T_g)_c$ are mostly due to experimental scatter.

high-velocity processes such as spray drying or pneumatic handling. Further work on the influence of the intensity of continuous mixing on the sticky-point is required to choose experimental conditions for specific applications when using the sticky-point test and the fluidized bed. Using the sticky-point test with a fluidized powder solves some of the issues of the individual methods. However, sensitive equipment is necessary to measure the smaller increase of torque at the sticky-point, compared to without fluidization, which is possible with advanced rheometers (Groen et al., 2020).

The cyclone test was proposed as an alternative for the fluidized bed test, while we expect it to achieve sufficient particle motion to be an alternative for the particle gun as well. Boonyai et al. (2004) suggested that the cyclone test's primary advantage over the fluidized bed is that the cyclone test measures both adhesion and cohesion while the fluidized bed measures only cohesion. Therefore, the cyclone test would be more suitable to predict stickiness in spray drying, fluidized beds, and pneumatic handling of powders (Boonyai et al., 2004). However, it is difficult to judge this statement since, besides the original paper by Boonyai et al. (2002), we only found one application of the cyclone test in literature (Intipunya et al., 2009).

The optical test can be used if the tested material scatters near-infrared light (Boonyai et al., 2004). Since it was proposed, no further experiments using this method have been reported to our knowledge. Hence, no judgment of its applicability can be made momentarily. Still, commonly tested powders such as amorphous lactose and various milk powders are all opaque, indicating that this method could be applied to these powders.

The most prominent application for the probe test is the droplet evaporation phase of spray drying. However, the use of a bulk moisture content severely limits this application. Werner et al. (2007a) measured the stickiness of an evaporating droplet with the probe test. The onset of stickiness occurred much earlier than expected based on the droplet's bulk moisture content, which indicated solute had accumulated at the droplet surface. Hence, the gravimetrically determined droplet water content is an unhelpful parameter for determining $T_2(x_w)$, which makes the probe test not applicable to industrial processes involving rapid evaporation. Crucially, this includes spray drying, for which there is no adequate method to predict droplet stickiness in the initial evaporation phase. Future methods should focus on the drying droplet's surface conditions for finding the tack point $T_2(x_w)$, either through direct measurement or by modeling the gradient formation under the influence of evaporation (Adhikari et al., 2005).

5. Conclusion

In this review, we provided an overview of methods that measure the stickiness of amorphous powders relevant in the food industry. The reviewed methods included visual observation tests, shear tests, the penetration test, the blow test, the sticky-point test, the fluidized bed, the particle gun, the cyclone test, the optical test, and the probe test. For each method, we described how either the sticky-point temperature $T_1(x_w)$ or the tack boundary $T_2(x_w)$ can be determined. We have classified the methods based on the particle mobility during the conditioning and measurement steps into *static stickiness tests* and *dynamic stickiness tests*.

Static stickiness tests have limited particle motion during the conditioning step, which can be as long as desired. Therefore, these tests are particularly suitable to measure the caking rate of powder beds. Hence, industrial applicability is predominantly in predicting the long-term behavior of powder during storage or in packaging. Static stickiness tests have shown that the caking rate can be related to $T - T_g$ when $T - T_g > (T - T_g)_c$, although the nature of the relation is dependent on the used method. Nonetheless, this approach gives much insight into the stability of stored powders.

Dynamic stickiness tests involve particles with significant particle motion during the conditioning and measurement step. The particle gun is a good method to measure stickiness during particle-wall impacts, while the combination of the sticky-point test and fluidized bed measure stickiness for particle-particle collisions and continuously mixed systems. A wide range of testing conditions can be achieved by varying the impact velocity or contact time between particles. Hence, information from dynamic stickiness tests is highly relevant to the design and operation of powder production and processing equipment. Dynamic stickiness tests have shown that velocity plays an important role in the location of the sticky region, with larger velocity shifting the sticky-point curve $T_1(x_w)$ to higher temperatures so that a larger $(T - T_g)_c$ is obtained.

An essential type of stickiness test that is lacking is a dynamic test that measures particle stickiness when moving from the liquid state to the sticky-region, hence, finding the tack boundary $T_2(x_w)$. Much unclarity exists for when evaporating solute containing droplets are sticky, while this is hugely relevant for spray drying, which is one of the most used processes in the food processing industry. The probe method does approach the sticky-region from the liquid state, but the reliance on the droplet's bulk properties makes it unable to determine values for $T_2(x_w)$. Further work in predicting the surface stickiness, either through direct measurement or by modeling the gradient formation under the influence of evaporation, is required to predict droplet stickiness.

Acknowledgments

This scientific work is supported by the Netherlands Organization for Scientific Research (NWO) (grant number 15459).

References

Adhikari B., Howes T., Lecomte D., Bhandari B.R., A glass transition temperature approach for the prediction of the surface stickiness of a drying droplet during spray drying, Powder Technology, 149 (2005) 168–179. DOI: 10.1016/j.powtec.2004.11.007

Adhikari B., Howes T., Shrestha A.K., Bhandari B.R., Development of stickiness of whey protein isolate and lactose droplets during convective drying, Chemical Engineering and Processing: Process Intensification, 46 (2007) 420–428. DOI: 10.1016/j.cep.2006.07.014

Aguilera J.M., Levi G., Karel M., Effect of water content on the glass transition and caking of fish protein hydrolyzates, Biotechnology Progress, 9 (1993) 651–654. DOI: 10.1021/bp00024a013

Anton Paar GmbH, 2020, Modular compact rheometer: MCR102/302/502, <www.anton-paar.com/corp-en/products/details/rheometer-mcr-102-302-502/> accessed 18.08.2020.

Bartels M., Lin W., Nijenhuis J., Kapteijn F., van Ommen J.R., Agglomeration in fluidized beds at high temperatures: mechanisms, detection and prevention, Progress in Energy and Combustion Science, 34 (2008) 633–666. DOI: 10.1016/j.pecs.2008.04.002

Billings S.W., Bronlund J.E., Paterson A.H.J., Effects of capillary condensation on the caking of bulk sucrose, Journal of Food Engineering, 77 (2006) 887–895. DOI: 10.1016/j.jfoodeng.2005.08.031

Boonyai P., Bhandari B.R., Howes T., Development of a novel testing device to characterize the sticky behavior of food powders-a preliminary study, in: Jindal V.K. (Ed.), Proceedings of the International Conference on Innovations in Food Processing Technology and Engineering, AIT, Bangkok, 11–13 December, 2002

Boonyai P., Bhandari B., Howes T., Stickiness measurement techniques for food powders: a review, Powder Technology, 145 (2004) 34–46. DOI: 10.1016/j.powtec.2004.04.039

Brennan J.G., Herrera J., Jowitt R., A study of some of the factors affecting the spray drying of concentrated orange juice, on a laboratory scale, International Journal of Food Science & Technology, 6 (1971) 295–307. DOI: 10.1111/j.1365-2621.1971.tb01618.x

Burnett D.J., Thielmann F., Booth J., Determining the critical relative humidity for moisture-induced phase transitions, International Journal of Pharmaceutics, 287 (2004) 123–133. DOI: 10.1016/j.ijpharm.2004.09.009

Chen J., Feng M., Gonzalez Y., Pugnaloni L.A., Application of probe tensile method for quantitative characterisation of the stickiness of fluid foods, Journal of Food Engineering, 87 (2008) 281–290. DOI: 10.1016/j.jfoodeng.2007.12.004

Chen X.D., Lake R., Jebson S., Study of milk powder deposition on a large industrial dryer, Food and Bioproducts Processing, 71 (1993) 180–186.

Dagdug L., García-Colín L.S., Generalization of the Williams–Landel–Ferry equation, Physica A: Statistical Mechanics and its Applications, 250 (1998) 133–141. DOI: 10.1016/S0378-4371(97)00542-6

Downton G.E., Flores-Luna J.L., King C.J., Mechanism of stickiness in hygroscopic, amorphous powders, Industrial & Engineering Chemistry Fundamentals, 21 (1982) 447–451. DOI: 10.1021/i100008a023

Ennis B.J., Tardos G., Pfeffer R., A microlevel-based characterization of granulation phenomena, Powder Technology, 65 (1991) 257–272. DOI: 10.1016/0032-5910(91)80189-P

Fabre A., Salameh S., Ciacchi L.C., Kreutzer M.T., van Ommen J.R., Contact mechanics of highly porous oxide nanoparticle agglomerates, Journal of Nanoparticle Research, 18 (2016) 200. DOI: 10.1007/s11051-016-3500-4

Ferry J.D., Viscoelastic Properties of Polymers, 3rd Edition, John Wiley & Sons, Inc., 1980, ISBN: 978-0-471-04894-7

Fitzpatrick J.J., Barry K., Cerqueira P.S.M., Iqbal T., O'Neill J., Roos Y.H., Effect of composition and storage conditions on the flowability of dairy powders, International Dairy Journal, 17 (2007a) 383–392. DOI: 10.1016/j.idairyj.2006.04.010

Fitzpatrick J.J., Hodnett M., Twomey M., Cerqueira P.S.M., O'Flynn J., Roos Y.H., Glass transition and the flowability and caking of powders containing amorphous lactose, Powder Technology, 178 (2007b) 119–128. DOI: 10.1016/j.powtec.2007.04.017

Fitzpatrick J.J., O'Callaghan E., O'Flynn J., Application of a novel cake strength tester for investigating caking of skim milk powder, Food and Bioproducts Processing, 86 (2008) 198–203. DOI: 10.1016/j.fbp.2007.10.009

Foster K.D., Bronlund J.E., Paterson A.H.J., The contribution of milk fat towards the caking of dairy powders, International Dairy Journal, 15 (2005) 85–91. DOI: 10.1016/j.idairyj.2004.05.005

Foster K.D., Bronlund J.E., Paterson A.H.J., Glass transition related cohesion of amorphous sugar powders, Journal of Food Engineering, 77 (2006) 997–1006. DOI: 10.1016/j.jfoodeng.2005.08.028

Freeman R., Measuring the flow properties of consolidated, conditioned and aerated powders — a comparative study using a powder rheometer and a rotational shear cell, Powder Technology, 174 (2007) 25–33. DOI: 10.1016/j.powtec.2006.10.016

Frenkel J., Viscous flow of crystalline bodies under the action of surface tension, Journal of Physics, 9 (1945) 385–391.

Green H., What is tack? Paper Trade Journal, 114 (1942) 39–42.

Groen J.C., Kooijman W., van Belzen D., Meesters G.M.H., Schütz D., Aschl T., Verolme P., Real-time in-situ rheological assessment of sticky point temperature and humidity of powdered products, KONA Powder and Particle Journal, 37 (2020) 176–186. DOI: 10.14356/kona.2020006

Hartmann M., Palzer S., Caking of amorphous powders — Material aspects, modelling and applications, Powder Technology, 206 (2011) 112–121. DOI: 10.1016/j.powtec.2010.04.014

Hammond J.F.H., Tack testing apparatus, US Patent, (1965)

US3214971A.

Hennigs C., Kockel T.K., Langrish T.A.G., New measurements of the sticky behavior of skim milk powder, Drying Technology, 19 (2001) 471–484. DOI: 10.1081/DRT-100103929

Hogan S.A., Famelart M.H., O'Callaghan D.J., Schuck P., A novel technique for determining glass–rubber transition in dairy powders, Journal of Food Engineering, 99 (2010) 76–82. DOI: 10.1016/j.jfoodeng.2010.01.040

Hogan S.A., O'Callaghan D.J., Influence of milk proteins on the development of lactose-induced stickiness in dairy powders, International Dairy Journal, 20 (2010) 212–221. DOI: 10.1016/j.idairyj.2009.11.002

Intipunya P., Shrestha A., Howes T., Bhandari B., A modified cyclone stickiness test for characterizing food powders, Journal of Food Engineering, 94 (2009) 300–306. DOI: 10.1016/j.jfoodeng.2009.03.024

Jenike A.W., Storage and flow of solids, bulletin no. 123, Bulletin of the University of Utah, 1964.

Kambe H., Kamagata K., A method of measuring tackiness, Journal of Applied Polymer Science, 13 (1969) 493–504. DOI: 10.1002/app.1969.070130310

Kamyabi M., Sotudeh-Gharebagh R., Zarghami R., Saleh K., Principles of viscous sintering in amorphous powders: a critical review, Chemical Engineering Research and Design, 125 (2017) 328–347. DOI: 10.1016/j.cherd.2017.06.009

Katkov I.I., Levine F., Prediction of the glass transition temperature of water solutions: comparison of different models, Cryobiology, 49 (2004) 62–82. DOI: 10.1016/j.cryobiol.2004.05.004

Khalkhali Z., Rothstein J.P., Characterization of the cold spray deposition of a wide variety of polymeric powders, Surface and Coatings Technology, 383 (2020) 125251. DOI: 10.1016/j.surfcoat.2019.125251

Knight P.C., Johnson S.H., Measurement of powder cohesive strength with a penetration test, Powder Technology, 54 (1988) 279–283. DOI: 10.1016/0032-5910(88)80058-5

Kudra T., Sticky region in drying—definition and identification, Drying Technology, 21 (2003) 1457–1469. DOI: 10.1081/DRT-120024678

Lazar M.E., Brown A.H., Smith G.S., Wang F.F., Lindquist F.E., Experimental production of tomato powder by spray drying. Food Technology, 3 (1956) 129–134.

Li R., Lin D., Roos Y.H., Miao S., Glass transition, structural relaxation and stability of spray-dried amorphous food solids: a review, Drying Technology, 37 (2019) 287–300. DOI: 10.1080/07373937.2018.1459680

Lockemann C.A., A new laboratory method to characterize the sticking properties of free-flowing solids, Chemical Engineering and Processing: Process Intensification, 38 (1999) 301–306. DOI: 10.1016/S0255-2701(99)00021-5

Lomellini P., Williams-Landel-Ferry versus Arrhenius behaviour: polystyrene melt viscoelasticity revised, Polymer, 33 (1992) 4983–4989. DOI: 10.1016/0032-3861(92)90049-3

Mitra H., Pushpadass H.A., Franklin M.E.E., Ambrose R.P.K., Ghoroi C., Battula S.N., Influence of moisture content on the flow properties of basundi mix, Powder Technology, 312 (2017) 133–143. DOI: 10.1016/j.powtec.2017.02.039

Murti R.A., Paterson A.H.J., Pearce D., Bronlund J.E., The influence of particle velocity on the stickiness of milk powder, International Dairy Journal, 20 (2010) 121–127. DOI: 10.1016/j.idairyj.2009.08.005

Özkan N., Walisinghe N., Chen X.D., Characterization of stickiness and cake formation in whole and skim milk powders, Journal of Food Engineering, 55 (2002) 293–303. DOI: 10.1016/S0260-8774(02)00104-8

Özkan N., Withy B., Dong Chen X., Effects of time, temperature, and pressure on the cake formation of milk powders, Journal of Food Engineering, 58 (2003) 355–361. DOI: 10.1016/S0260-8774(02)00419-3

Palzer S., The effect of glass transition on the desired and undesired agglomeration of amorphous food powders, Chemical Engineering Science, 60 (2005) 3959–3968. DOI: 10.1016/j.ces.2005.02.015

Palzer S., Zürcher U., Kinetik unerwünschter Agglomerationsprozesse bei der Lagerung und Verarbeitung amorpher Lebensmittelpulver, Chemie Ingenieur Technik, 76 (2004) 1594–1599. DOI: 10.1002/cite.200407009

Papadakis S.E., Bahu R.E., The sticky issues of drying, Drying Technology, 10 (1992) 817–837. DOI: 10.1080/07373939208916484

Pasley H., Haloulos P., Ledig S., Stickiness – a comparison of test methods and characterisation parameters, Drying Technology, 13 (1995) 1587–1601. DOI: 10.1080/07373939508917041

Paterson A.H.J., Bronlund J.E., Brooks G.F. The blow test for measuring the stickiness of powders, in AIChE 2001 Annual Meeting, 2001.

Paterson A.H., Bronlund J.E., Zuo J.Y., Chatterjee R., Analysis of particle-gun-derived dairy powder stickiness curves, International Dairy Journal, 17 (2007a) 860–865. DOI: 10.1016/j.idairyj.2006.08.013

Paterson A.H.J., Brooks G.F., Bronlund J.E., Foster K.D., Development of stickiness in amorphous lactose at constant T–Tg levels, International Dairy Journal, 15 (2005) 513–519. DOI: 10.1016/j.idairyj.2004.08.012

Paterson A.H.J., Ripberger G.D., Bridges R.P., Measurement of the viscosity of freeze dried amorphous lactose near the glass transition temperature, International Dairy Journal, 43 (2015) 27–32. DOI: 10.1016/j.idairyj.2014.11.005

Paterson A.H., Zuo J.Y., Bronlund J.E., Chatterjee R., Stickiness curves of high fat dairy powders using the particle gun, International Dairy Journal, 17 (2007b) 998–1005. DOI: 10.1016/j.idairyj.2006.11.001

Peleg M., On the use of the WLF model in polymers and foods, Critical Reviews in Food Science and Nutrition, 32 (1992) 59–66. DOI: 10.1080/10408399209527580

Roos Y.H., Importance of glass transition and water activity to spray drying and stability of dairy powders, Lait, 82 (2002) 475–484. DOI: 10.1051/lait:2002025

Roos Y.H., Glass transition temperature and its relevance in food processing, Annual Review of Food Science and Technology, 1 (2010) 469–496. DOI: 10.1146/annurev.food.102308.124139

Schulnies F., Kleinschmidt T., Time consolidation of skim milk powder near the glass transition temperature, International Dairy Journal, 85 (2018) 105–111. DOI: 10.1016/j.idairyj.2018.05.005

Schulze D., Powders and Bulk Solids: Behavior, Characterization, Storage and Flow, Springer, 2008, ISBN: 978-3-540-73767-4. DOI: 10.1007/978-3-540-73768-1

Schutyser M.A.I., Both E.M., Siemons I., Vaessen E.M.J., Zhang L., Gaining insight on spray drying behavior of foods via single droplet drying analyses, Drying Technology, 37 (2019) 525–534. DOI: 10.1080/07373937.2018.1482908

Schwedes J., Review on testers for measuring flow properties of bulk solids, Granular Matter, 5 (2003) 1–43. DOI: 10.1007/s10035-002-0124-4

Seville J.P.K., Willett C.D., Knight P.C., Interparticle forces in fluidisation: a review, Powder Technology, 113 (2000) 261–268. DOI: 10.1016/S0032-5910(00)00309-0

Simha R., Boyer R.F., On a general relation involving the glass temperature and coefficients of expansion of polymers, The Journal of Chemical Physics, 37 (1962) 1003–1007. DOI: 10.1063/1.1733201

Sochava I.V., Heat capacity and thermodynamic characteristics of denaturation and glass transition of hydrated and anhydrous proteins, Biophysical Chemistry, 69 (1997) 31–41. DOI: 10.1016/S0301-4622(97)00072-0

Tsourouflis S., Flink J.M., Karel M., Loss of structure in freeze-dried carbohydrates solutions: effect of temperature, moisture content and composition, Journal of the Science of Food and Agriculture, 27 (1976) 509–519. DOI: 10.1002/jsfa.2740270604

van der Knaap J., On-line monitoring of dynamic stickiness and particle size distribution in a fluidized bed dryer by attractor comparison, MSc thesis, Delft University of Technology, 2006.

Van Ommen J.R., Monitoring fluidized bed hydrodynamics, Doctoral dissertation, Delft University of Technology, 2001.

Verdurmen R.E.M., van Houwelingen G., Gunsing M., Verschueren M., Straatsma J., Agglomeration in spray drying installations (the EDECAD project): stickiness measurements and simulation results, Drying Technology, 24 (2006) 721–726. DOI: 10.1080/07373930600684973

Verschueren M., Verdurmen R.E.M., van Houwelingen G., Backx A.C.P.M., van der Knaap J.E.A., Bartels M., van Ommen J.R., Dynamic stickiness measurements by attractor comparison: a feasibility study, in Proc. Int. Conf. Liquid Atomisation and Spray Systems (ICLASS), Kyoto, Japan Aug 27–Sept 1, 2007.

Wallack D.A., King C.J., Sticking and agglomeration of hygroscopic, amorphous carbohydrate and food powders, Biotechnology Progress, 4 (1988) 31–35. DOI: 10.1002/btpr.5420040106

Walmsley T.G., Walmsley M.R.W., Atkins M.J., Neale J.R., Analysis of skim milk powder deposition on stainless steel tubes in cross-flow, Applied Thermal Engineering, 75 (2015) 941–949. DOI: 10.1016/j.applthermaleng.2014.10.066

Walmsley T.G., Walmsley M.R.W., Atkins M.J., Neale J.R., Sellers C.M., An experimentally validated criterion for skim milk powder deposition on stainless steel surfaces, Journal of Food Engineering, 127 (2014) 111–119. DOI: 10.1016/j.jfoodeng.2013.11.025

Werner S.R.L., Jones J.R., Paterson A.H.J., Stickiness during drying of amorphous skin-forming solutions using a probe tack test, Journal of Food Engineering, 81 (2007a) 647–656. DOI: 10.1016/j.jfoodeng.2006.12.008

Werner S.R.L., Jones J.R., Paterson A.H.J., Stickiness of maltodextrins using probe tack test during in-situ drying, Journal of Food Engineering, 80 (2007b) 859–868. DOI: 10.1016/j.jfoodeng.2006.08.008

Williams M.L., Landel R.F., Ferry J.D., The temperature dependence of relaxation mechanisms in amorphous polymers and other glass-forming liquids, Journal of the American Chemical Society, 77 (1955) 3701–3707. DOI: 10.1021/ja01619a008

Zhao S., Experimental and numerical investigations of skim milk powder stickiness and deposition mechanisms, MSc Thesis, University of Waikato, 2009.

Zuo J.Y., The stickiness curve of dairy powders, M. Tech. thesis, Massey University, 2004.

Zuo J.Y., Paterson A.H., Bronlund J.E., Chatterjee R., Using a particle-gun to measure initiation of stickiness of dairy powders, International Dairy Journal, 17 (2007) 268–273. DOI: 10.1016/j.idairyj.2006.02.010

Authors' Short Biographies

Erik J.G. Sewalt

Erik Sewalt MSc obtained his MSc in Food Technology at Wageningen University & Research. His specialization was Sustainable Food Process Engineering. His MSc thesis was about modeling the diffusion of pepsin in protein gels to understand food breakdown. He did an internship on in-vitro digestion of protein-rich food at University of California, Davis, USA. From October 2017, he became a PhD candidate at TU Delft, Faculty of Applied Sciences, Product and Process Engineering. His research activities as PhD candidate revolve around understanding the agglomeration of evaporating droplets in spray drying.

Authors' Short Biographies

Fuweng Zhang

Dr. Fuweng Zhang is a postdoc working at Dept. Chemical Engineering, Delft University of Technology (the Netherlands). He received his Ph.D. from the University of Sciences and Technology Beijing in 2014. After that, he was appointed as a post-doctoral researcher working at University College Cork, Ireland. He has 6 years of experience in the research area of multi-phase flow, pneumatic transportation, and fluidization of powder materials. He currently focuses his research on developing novel technologies to enhance the fluidization of the cohesive pharmaceutical powders.

Volkert van Steijn

Assistant Professor at the Department of Chemical Engineering at Delft University of Technology (the Netherlands). He obtained his PhD degree on droplet microfluidics in 2010, with honours. He worked as a postdoc at Harvard University in the lab of Prof. David Weitz on the development of droplet-based laboratories-on-a-chip for applications in the area of life sciences. With a strong background in soft matter, droplet flows, and transport phenomena, his group develops microfluidic tools that contribute to solving problems in the area of health and life sciences.

J. Ruud van Ommen

Professor of Chemical Enginering at Delft University of Technology (the Netherlands). He obtained his PhD degree at Delft in 2001. He has been visiting professor at Chalmers University of Technology (Gothenburg, Sweden) and the University of Colorado (Boulder, USA). In recent years, he expanded his research from chemical reactor engineering to the scalable production of advanced, nanostructured materials. In 2011, he started an ambitious program (funded by an ERC Starting Grant) to investigate the interplay between agglomeration and coating of nanoparticles in the gas phase. He has published about 200 journal papers, of which a considerable part on powder technology.

Gabrie M.H. Meesters

Dr Gabrie Meesters has 27 years of industrial formulations experience at Gistbrocades, Genencor International and DSM. He has 23 years of experience as a part-time professor at TU Delft in particle technology and product design. From January 2019, he became a full-time assistant professor at the TU Delft, Faculty of Applied Sciences, Product and Process Engineering. He is a contributor to several books on formulation. He is the editor of three books on product design and solids processing. He published over 70 refereed papers, has more than 20 patents and supervised more than 100 BSc, MSc and PhDs. He is a regular speaker at conferences and workshops. He was the organizer of the 2010 Partec and the 2010 World Congress on Particle Technology in Nuremberg, Germany.